

Degranulation of Paneth Cells via Toll-Like Receptor 9

Cristiano Rumio,* Dario Besusso,[†]
Marco Palazzo,* Silvia Selleri,* Lucia Sfondrini,[†]
Francesco Dubini,[‡] Sylvie Ménard,[†] and
Andrea Balsari[§]

From the Department of Human Morphology* and the Institutes of Microbiology[‡] and Pathology,[§] University of Milan, Milan; and the Molecular Targeting Unit,[†] Istituto Nazionale Tumori, Milan, Italy

The release of antimicrobial peptides and growth factors by Paneth cells is thought to play an important role in protecting the small intestine, but the mechanisms involved have remained obscure. Immunohistochemistry and immunofluorescence showed that Paneth cells express Toll-like receptor 9 (TLR9) in the granules. Injection of mice with oligonucleotides containing CpG sequence (CpG-ODNs) led to a down-modulation of TLR9 and a striking decrease in the number of large secretory granules, consistent with degranulation. Moreover CpG-ODN treatment increased resistance to oral challenge with virulent *Salmonella typhimurium*. Moreover, our findings demonstrate a sentinel role for Paneth cells through TLR9. (*Am J Pathol* 2004, 165:373–381)

The primary role of the small intestine is the digestion of food into low-molecular mass components, followed by their absorption. The absorptive surface of the intestine is covered with a carpet of villi, surrounded by very narrow pits, or crypts. At the bottom of each small intestinal crypt is a cluster of 5 to 15 Paneth cells. These are pyramidally shaped epithelial cells filled with numerous cytoplasmic granules^{1–4} containing an array of antimicrobial molecules such as defensins^{5,6} (termed cryptidins), lysozyme,^{7,8} and type II phospholipase A2.⁹ Electron microscopic observations have localized secretory granules and smooth-surfaced vesicles in the apical cytoplasm, while an oval nucleus is located in the basal cytoplasm.¹⁰ The presence of multiple antibacterial proteins in the secretory granules of Paneth cells has led to the hypothesis that these cells sense bacteria entering the crypt, and respond by releasing antimicrobial substances. The resulting increased concentration of antimicrobial molecules in the intestinal lumen may be important in controlling microbial density in the small intestine where microbial nutrients in the form of digests are plentiful. Moreover, the vital processes of small intestinal epithelial cell renewal take place in the crypts, and Paneth cells located at the base of these crypts have been impli-

cated in these processes because the cells produce intestinal trefoil factor¹¹ that promotes cell migration; epidermal growth factor¹² that stimulates the growth of epithelial cells; and osteopontin, a regulator of cell-matrix interaction, cell polarization, and cell migration.¹³ Thus, current evidence supports an important role for Paneth cells in the defense against pathogens, in the regulation of microbial density in the small intestine, and in the protection and regulation of nearby stem cells. Paneth cell granule release in response to microbial products^{10,14–19} has been recently confirmed by Ayabe and colleagues²⁰ using *in vitro* isolated intact crypts. However the receptors that allow Paneth cells to sense bacteria have remained unknown. The simplest scenario would place the receptors directly on the Paneth cells, but it is also possible that other crypt cells sense bacteria and relay the signal to the bottom of the crypt by cell-to-cell communication or via soluble mediators.

Toll-like receptors (TLRs), which are mammalian homologs of the *Drosophila* protein Toll²¹ involved in anti-fungal defense,²² are part of the innate immune response to microbial pathogens.²³ Recent studies had provided evidence that TLR9 recognizes bacterial DNA, in particular sequences containing unmethylated CpG dinucleotides. Indeed bacterial DNA or synthetic CpG-motif-containing oligodeoxynucleotides (CpG-ODNs) applied directly to B cells, macrophages, and dendritic cells result in the release of a plethora of predominantly Th-1-associated cytokines.^{24,25} Very recently, human colonic epithelial cell lines were shown to express TLR9 and to respond to *Escherichia coli* DNA or CpG-ODNs by increased interleukin-8 production.²⁶

Here, we report the expression of TLR9 in Paneth cells of mouse and human small intestine and the down-modulation of TLR9 in these cells, accompanied by a striking decrease in the number of large secretory granules and the formation of large vacuoles, after *in vivo* exposure to CpG-ODNs. Moreover, pretreatment of mice with CpG-ODNs increases resistance to oral challenge with virulent *Salmonella typhimurium*.

Partially supported by the Associazione Italiana per la Ricerca sul Cancro and Finanziamenti per L'Innovazione, La Ricerca e lo Sviluppo Tecnologico (FIRST).

C.R. and D.B. contributed equally to this work.

Accepted for publication April 1, 2004.

Address reprint requests to Prof. Andrea Balsari, Chair of Immunology c/o Molecular Targeting Unit, Dept. of Experimental Oncology, Istituto Nazionale Tumori, Via Venezian 1, 20133 Milan, Italy. E-mail: andrea.balsari@unimi.it.

Materials and Methods

Reagents

Purified single-stranded 1668 CpG-ODN (5'-TCCAT-GACGTTC CTGATGCT-3') containing a CpG motif and control AP1-ODN (5'-GCTTGATGACTCAGCCGAA) lacking a CpG motif were synthesized by M-Medical-Genenco (Firenze, Italy) under endotoxin-free conditions and dissolved in sterile water. Both ODNs were phosphorothioated to reduce the susceptibility of the ODNs to DNase digestion, thereby significantly prolonging their half-life *in vivo*. Goat anti-human TLR9 N-15 was purchased from Santa Cruz Biotechnology (Santa Cruz, CA). Murine biotinylated anti-murine TLR9 monoclonal antibody (mAb) 5G5 was purchased from Hycult Biotechnology b.v. (Uden, The Netherlands).

Western Blot Analysis

Cell extracts were prepared from human colorectal adenocarcinoma HT-29 [American Type Culture Collection (ATCC), Rockville, MD], human embryonic kidney HEK293 (ATCC), murine T lymphoma EL-4 (ATCC), and B lymphocytes, obtained from freshly isolated splenocytes by magnetic cell sorting using anti-CD19 microbeads (Miltenyi Biotec, Bologna, Italy), by lysis in 50 mmol/L Tris-HCl, 150 mmol/L NaCl, 1% Nonidet P-40, 10 μ g/ml aprotinin, 10 μ g/ml leupeptin, and 10 mmol/L phenylmethyl sulfonyl fluoride for 1 hour at 4°C, followed by centrifugation. Samples were mixed with NuPage LDS sample buffer and NuPage sample reducing agent (both from Invitrogen Italia, Milan, Italy) and boiled for 10 minutes at 70°C. Total cell lysates (50 μ g/lane) were subjected to 10% sodium dodecyl sulfate-polyacrylamide gel electrophoresis (Invitrogen) and transferred to nitrocellulose membranes. After blocking, membranes loaded with human and murine cell extracts were exposed to the respective anti-human and anti-murine TLR9 reagents, washed, and incubated with peroxidase-conjugated rabbit anti-goat IgG and peroxidase-conjugated streptavidin, respectively. Membranes were washed and developed by enhanced chemiluminescence (Amersham Bioscience, Milan, Italy) according to the manufacturer's instructions.

Bacteria

S. typhimurium, strain ATCC 14028, was grown in BHI broth (Becton Dickinson, Palo Alto, CA), supplemented with 10% fetal calf serum (Seromed, Berlin, Germany). *S. typhimurium* was passaged twice in C57BL/6 mice by oral inoculation to enhance virulence. Bacteria were isolated from the orally infected mice by washing the peritoneum with 1 ml of saline. The collected liquid was plated on selective agar (Becton Dickinson). Bacterial stocks were stored in aliquots at -70°C. Bacteria used for inoculation were grown to log phase in brain heart infusion (BHI) broth and diluted to obtain the appropriate concentration of bacteria, determined by optical density at 600 nm. The

actual inoculation titer [number of colony-forming units (CFU)] was measured by plating serial dilutions.

Mice

FVB and C57BL/6 mice were purchased from Charles River (Calco, Italy) and used at 8 to 12 and 4 to 6 weeks of age, respectively. C57BL/6 mice used for *S. typhimurium* infection were maintained under specific pathogen-free conditions. Experimental protocols were approved by the Ethics Committee for Animal Experimentation of the Istituto Nazionale Tumori di Milan, according to United Kingdom Co-ordinating Committee on Cancer Research guidelines.²⁷

Preparation of Small Intestine Crypts and Northern Blot Analysis

Intestinal crypts from mice injected intraperitoneally 3 hours previously with 40 μ g of CpG-ODN or saline were isolated by ethylenediaminetetraacetic acid dissociation of small intestine segments as described by Arabe and colleagues.²⁰ Briefly, segments of second half of mouse small intestine were averted and shaken in Ca⁺⁺-Mg⁺⁺-free phosphate-buffered saline (PBS) buffer containing 30 mmol/L ethylenediaminetetraacetic acid to elute crypts. Villi and crypts eluted during 5-minute intervals were deposited by centrifugation at 700 \times g and resuspended in PBS buffer. Total RNA was extracted from isolated crypts and 5 μ g of RNA from each mouse was fractionated by formaldehyde-agarose gel electrophoresis and then blotted onto a nylon membrane (Hybond N+, Amersham Bioscience). Northern blots were sequentially hybridized to cryptdin 1 (CAGCCTGGACCTGGAA-GGCCAGCAGGACAAGGGCAGAGAGGAGGACTA) and GAPDH (full-length coding sequence) ³²P-labeled probes. Hybridizations were done overnight at 37°C in 50% formamide and washed at room temperature for 1 hour, followed by washing at 55°C in 2 \times standard saline citrate (1 \times standard saline citrate is 0.15 mol/L NaCl plus 0.015 mol/L sodium citrate)-0.1% sodium dodecyl sulfate. Northern blots were scanned and the band intensity was determined by the ImageQuant program (Molecular Dynamics, Sunnyvale, CA). Band intensity for cryptdin 1 was expressed as a proportion of the GAPDH value.

Immunohistochemistry and Immunofluorescence

TLR9 expression was assessed on normal intestine specimens obtained from surgical cancer patients of Istituto Nazionale Tumori and from FVB mice. Samples were fixed immediately in 10% neutral buffered formalin for 4 hours and embedded in paraffin. For immunohistochemistry, paraffin specimens were sectioned at 5 μ m and collected on silanized slides, deparaffinized, and rinsed in Tris-HCl. After antigen retrieval by autoclaving in 0.01 mol/L (pH 6) sodium citrate and after quenching of endogenous peroxidase in 0.3% H₂O₂ in 0.1 mol/L Tris-

HCl for 20 minutes, nonspecific sites were blocked with following solution, 0.05 mol/L Tris-HCl, 0.15 mol/L NaCl, 0.5% ovalbumin, 0.1% gelatin, 0.05% Tween 20, and 0.2% fish gelatin for 20 minutes at room temperature. Murine and human sections were incubated with anti-mouse TLR9 5G5 and with anti-human TLR9 N-15 antibodies, respectively, for 1 hour at 37°C. TLR9 5G5 was detected by ABC Elite Vectastain (Vector Laboratories, Burlingame, CA) and TLR9 N-15 was detected by biotinylated rabbit anti-goat immunoglobulins and peroxidase-conjugated streptavidin (DAKO, Carpinteria, CA) (diluted 1:100 and 1:300 in PBS). Sections were then mounted in entellan.

For immunofluorescence, antigen retrieval was performed and murine sections were incubated with 0.1 mol/L glycine buffer for 5 minutes at room temperature. Nonspecific sites were blocked with a solution of 0.05 mol/L Tris-HCl, 0.15 mol/L NaCl, 0.5% ovalbumin, 0.1% gelatin, 0.05% Tween 20, and 0.2% fish gelatin for 20 minutes at room temperature, and slides were incubated with anti-TLR9 5G5 antibody for 1 hour at 37°C. After rinsing, sections were incubated with tetramethyl-rhodamine isothiocyanate-conjugated streptavidin (Jackson ImmunoResearch Laboratories, Inc., West Grove, PA) at a 1:1000 dilution in Tris-HCl for 30 minutes at 37°C. Nuclei were counterstained with YoPro-1 (Molecular Probes, Eugene, OR) and slides were mounted with Mowiol mounting medium. TLR9 immunofluorescence was observed under a confocal laser-scanning microscope (MicroRadiance 2100; Bio-Rad) mounted on an inverted microscope (Nikon Eclipse 300). Illumination sources were an argon laser (488 nm) to excite YoPro-1 and He-Ne (543 nm) for tetramethyl-rhodamine isothiocyanate. Single channels were collected sequentially using a selective barrier filter detecting green fluorescence to cut off the possible emission of the second peak of tetramethyl-rhodamine isothiocyanate at 514 nm. All images were collected using a PlanApo 60 × 1.4 NA oil immersion lens, at 512 × 512 pixels and a scanning time of 1 second. Projection images were obtained from serial optical sections using LaserSharp software (Bio-Rad).

In Vivo Studies

Intestinal expression of TLR9 was analyzed in mice (four animals/group) either untreated or injected intraperitoneally 24 hours before with 1668 CpG-ODN or control AP1-ODN at a dose of 40 μg/mouse. TLR9-stained granules in Paneth cells were quantitated only in crypts sectioned through the center and revealing a clear lumen. Five crypts were analyzed for each mouse. For each crypt, the ratio of number of TLR9-stained granules to number of Paneth cells was calculated. From the five measurements of the four mice of each group, mean values of TLR9-positive granules per cell were compared using Student's *t*-test.

Depletion of secretory granules from Paneth cells after CpG-ODN treatment was analyzed by optic and electron microscopy of crypts obtained from mice (two animals/group) either untreated or injected intraperitoneally 24

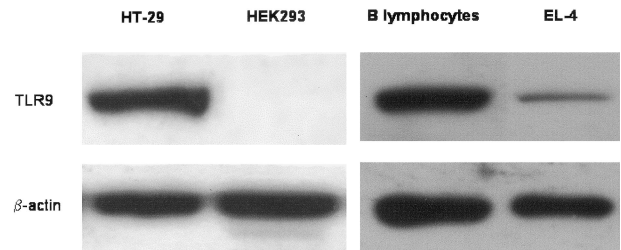


Figure 1. Western blot analysis of murine B lymphocyte and EL-4 cell lysates (**right**) and human HT-29 and HEK293 cell lysates (**left**) using antibodies 5G5 and N-15 against murine TLR9 and human TLR9, respectively.

hours, 12 hours, and 3 hours previously with 1668 CpG- or control AP1-ODNs at a dose of 40 μg/mouse. Jejunum fragments were removed and processed as above. For each mouse five to six microislets were fixed in 3.3% glutaraldehyde in 0.1 mol/L phosphate buffer (pH 7.4) for 2 hours at 4°C, washed in 0.1 mol/L phosphate buffer, postfixed in 1% osmium tetroxide in 0.1 mol/L phosphate buffer, dehydrated through an ascending series of ethanols, and embedded in Araldite. Ultra-thin sections were cut on a diamond knife with a Reichert Ultracut R ultramicrotome (Leica, Wien, Austria), stained with uranyl acetate and lead citrate, and observed with a Jeol CX100 transmission electron microscope (Jeol, Tokyo, Japan). Semithin sections from the some samples were analyzed by an optical microscopy Nikon 600 equipped with a digital camera Nikon DXR 1200 (Nikon, Tokyo, Japan).

Bacterial infection was analyzed in C57BL/6 mice maintained under specific pathogen-free conditions. Mice were treated with 1668 CpG-ODN intraperitoneally at a dose of 40 μg/200 μl saline (20 animals) or with saline alone (10 animals). Three days after, mice of each treatment were randomly divided in two groups and 1.6×10^5 or 1.6×10^7 CFU of *S. typhimurium* in 0.3 ml was orally inoculated using a syringe fitted with a feeding needle. The number of dead animals was recorded daily.

Results

Expression of TLR9 in Murine and Human Intestine

Western immunoblotting confirmed the specificity of two commercially available anti-murine and anti-human TLR9 antibodies. The anti-murine TLR9 mAb 5G5 detected a protein of the appropriate molecular weight in murine B lymphocytes, whereas EL-4 T cells showed a faint band (Figure 1, right), in keeping with the reported high and low TLR9 mRNA expression in B and T cells, respectively.²⁸ The anti-human TLR9 N-15 antibody detected an immunoreactive protein at the appropriate molecular weight in human HT-29 colon cells but not in HEK-293 kidney cells (Figure 1, left), described as TLR9-positive and TLR9-negative cell lines, respectively, based on reverse transcriptase-polymerase chain reaction analysis.^{26,29}

Immunohistochemical staining of transverse sections of murine small intestine with mAb 5G5 indicated expression of TLR9 in the cytoplasm of enterocytes of the villi

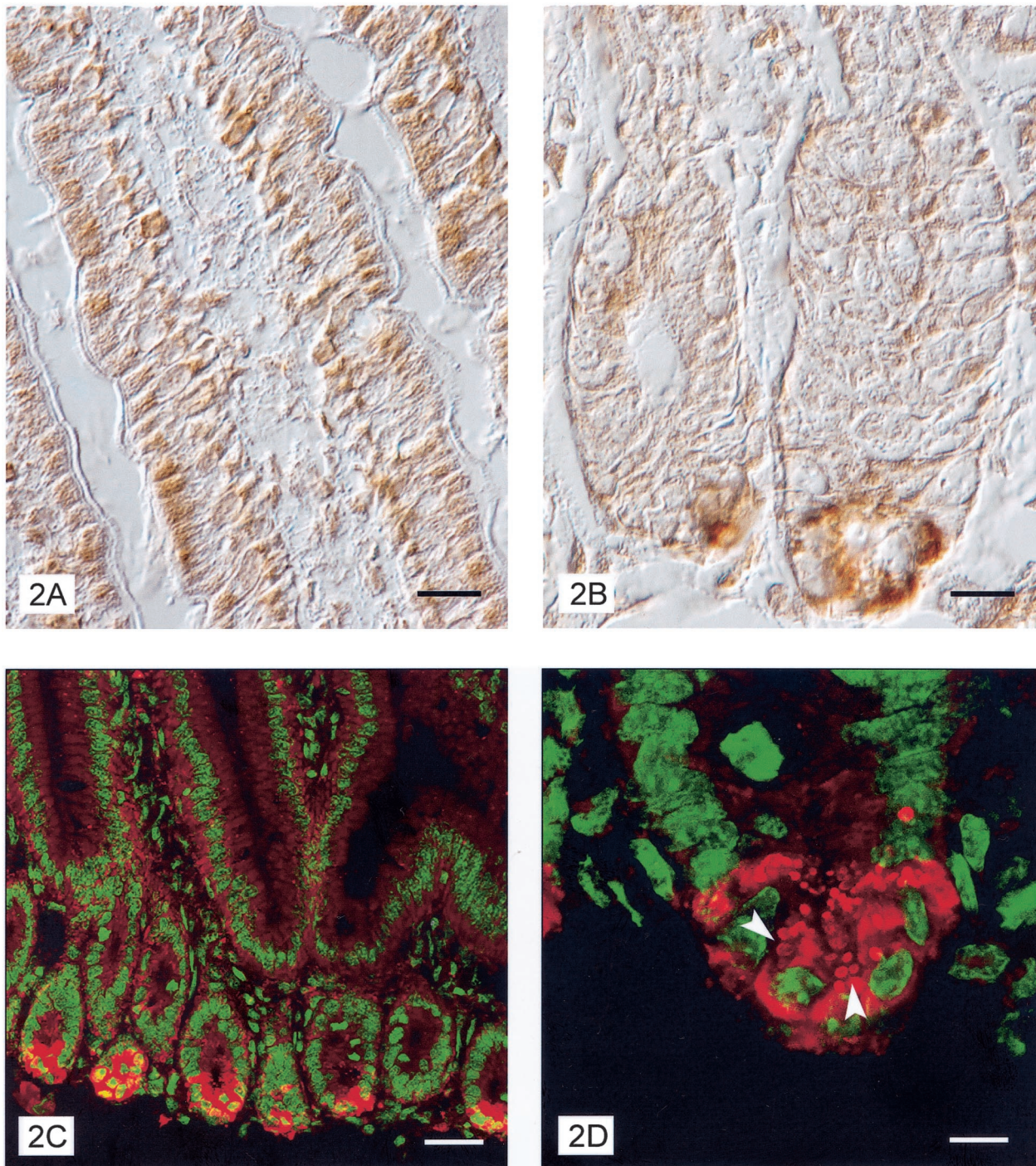


Figure 2. Interference contrast images of villi longitudinal sections from murine jejunum immunostained with anti-TLR9 mAb 5G5 show expression of TLR9 in cytoplasm of enterocytes (**A**) and in Paneth cells (**B**). Confocal microscope images of TLR9 expression in enterocytes and Paneth cells (**C**) with granules (**arrowhead**) clearly labeled (**D**). Red, TLR9 staining; green, Yopro-3 nuclear staining. Scale bars: 10 μ m (**A**, **B**); 30 μ m (**C**); 8 μ m (**D**).

and crypts (Figure 2A). Staining was localized in small dots. Sporadic labeled cells, probably leukocytes, were observed in the lamina propria. Note that TLR9 staining was more intense at the level of Paneth cells, in deeper parts of the crypts where these cells reside (Figure 2B). In these cells, labeling was compartmentalized in large

dots. Confocal microscopy confirmed the immunohistochemical results and demonstrated the localization of TLR9 mainly in the secretory granules (Figure 2, C and D). Immunohistochemical analysis of human transverse ileum sections using the anti-human TLR9 N-15 polyclonal antibody also revealed enterocyte and Paneth cell

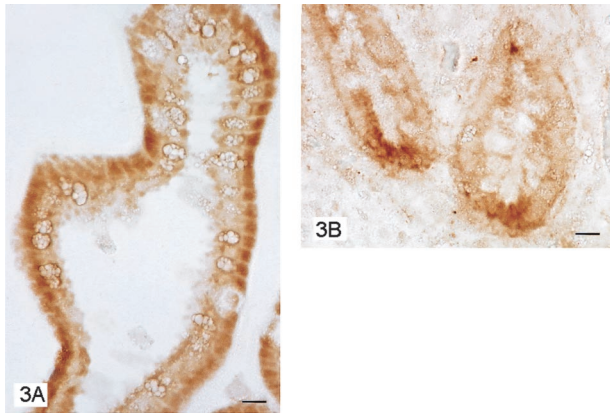


Figure 3. Photomicrographs of transverse section of human ileum. Enterocytes labeled with N-15 antibody against TLR9 (**A**). Detail of the deep portion of ileum mucosa with Paneth cells strongly labeled (**B**). Scale bars, 10 μ m.

staining. Again, labeling was confined to and localized in the cytoplasm of enterocytes and Paneth cells, with more intense staining in the latter (Figure 3, A and B).

Down-Regulated Expression of TLR9 in Intestine of CpG-ODN-Treated Mice

Mice were treated intraperitoneally with CpG-ODNs, control AP1-ODNs, or left untreated, and jejunum sections prepared for immunohistochemistry 24 hours later. Staining with anti-murine TLR9 5G5 mAb revealed a decrease in the TLR9 expression in enterocytes, especially in Paneth cells, of CpG-ODN-treated mice (Figure 4A), whereas staining in sections from AP1-ODN-treated and untreated mice showed no detectable difference (Figure 4, B and C). Confocal microscopy revealed a marked reduction in the number of stained granules in Paneth cells (Figure 4; D to F). Indeed, 6.38 ± 0.78 and 5.78 ± 0.85 (mean \pm SD) TLR9-positive granules per cell were detected in untreated and control ODN-treated mice, respectively, whereas only 2.20 ± 0.36 granules were observed in the CpG-ODN-treated mice ($P < 0.001$ Student's *t*-test).

Depletion of Secretory Granules from Paneth Cells after CpG-ODN Treatment

To determine whether down-modulation of TLR9 in Paneth cells of CpG-ODN-treated mice resulted from degranulation of these cells, secretory granules from mice untreated or injected intraperitoneally with 1668 CpG-ODN or control AP1-ODN 24 hours, 12 hours, and 3 hours previously were analyzed by optic and electron microscopy. In untreated and AP1-treated mice, light microscopy showed Paneth cells filled with large granules (Figure 5A), which by electron microscopy are revealed as an electron-dense core surrounded by a small clear crown (Figure 5B). In Paneth cells 3 hours after treatment of mice with CpG-ODNs, the size of granules was dramatically decreased as compared with those in AP1-treated or control mice, and the granules were localized toward the apical cell membrane (Figure 5, C and D). Some

fields revealed portions of granules (half-moon shape) filled with electron-dense material, suggestive of granule fragments (inset in Figure 5D). Some Paneth cells of mice treated 12 hours before with CpG-ODNs showed a decreased diameter of secretory granules whereas in other granules, the dimensions were similar to those in untreated and AP1-treated mice; frequently one or more large membrane-limited vacuoles, surrounded by small vesicles, were present (Figure 5, E and F). Paneth cells of mice treated 24 hours before with CpG-ODNs showed morphology similar to that of control cells (data not shown).

mRNA Expression of Paneth Cell Cryptdin 1 in Response to CpG-ODN

The effect of CpG-ODN treatment on Paneth cell antimicrobial mRNA expression was analyzed in intestinal crypts isolated from mice injected intraperitoneally 3 hours previously with 40 μ g of CpG-ODN or saline. Paneth cells from mice pretreated with CpG-ODN revealed on average, an increase in cryptdin 1 mRNA expression (Figure 6).

Effect of CpG-ODN Treatment on Lethal Infection with S. typhimurium

Defensins and other polypeptides secreted by Paneth cells are thought to contribute to host defense of the small intestine. In support of this hypothesis, studies in matrilysin-deficient mice lacking mature defensins³⁰ and in transgenic mice expressing a human intestinal defensin¹⁸ demonstrated a role for defensins *in vivo* against oral challenge with *S. typhimurium*. We assessed the survival of mice treated intraperitoneally with CpG-ODN or saline and 72 hours later, inoculated with 1.6×10^5 or 1.6×10^7 CFU of a virulent strain of *S. typhimurium*. At both doses of bacterial inoculum, mice pretreated with CpG-ODN survived longer to *S. typhimurium* infection than did mice treated with saline alone ($P = 0.0289$ and $P = 0.0014$, respectively, by log-rank test) (Figure 7).

Discussion

The present study demonstrates the expression of the TLR9 protein in normal gut epithelial cells, extending the list of TLRs found in intestinal epithelia and supporting a sentinel role for intestinal cells.³¹ Although quantitative definition and comparison of differential TLR expression based on immunohistochemistry is difficult, TLR9 appears to be constitutively expressed by intestinal epithelial cells of normal mucosa as reported for TLR3 and TLR5, whereas TLR2 and TLR4 expression has been described as very low level.³²

Our results also provide the first evidence of high-level TLR9 expression in Paneth cells, localized mainly at the level of secretory granules, as shown by confocal microscopy. These observations indicate a way by which Paneth cells sense the presence of bacterially derived mol-

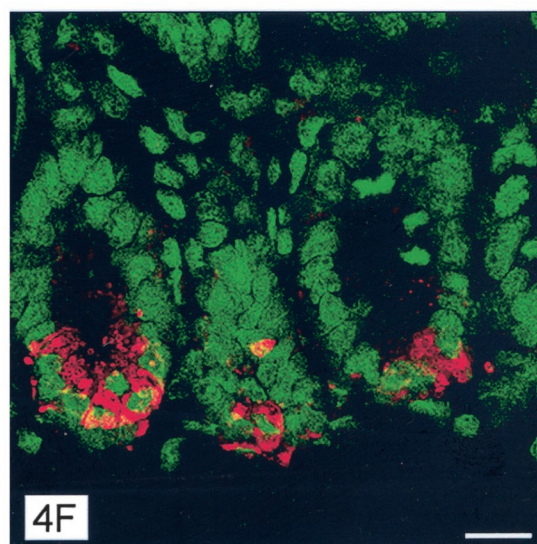
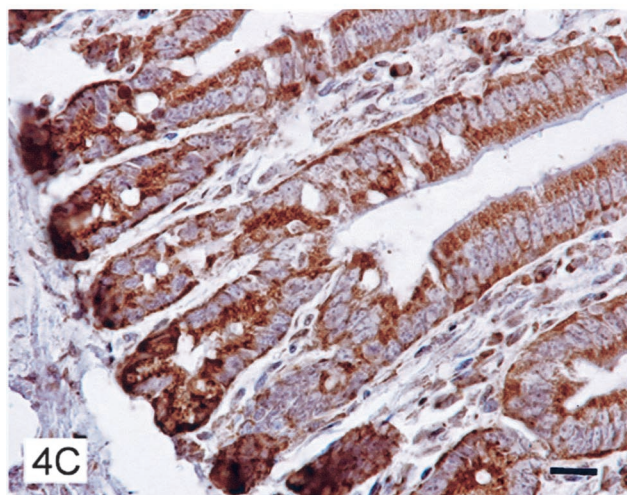
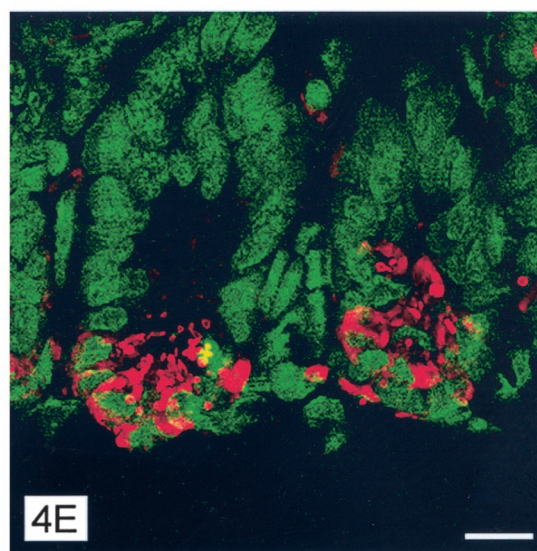
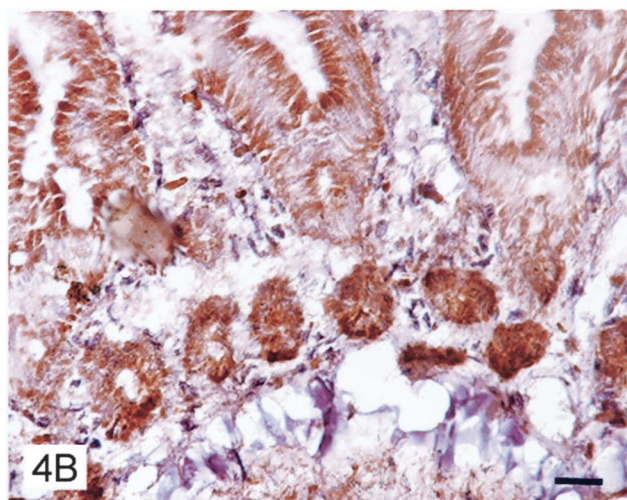
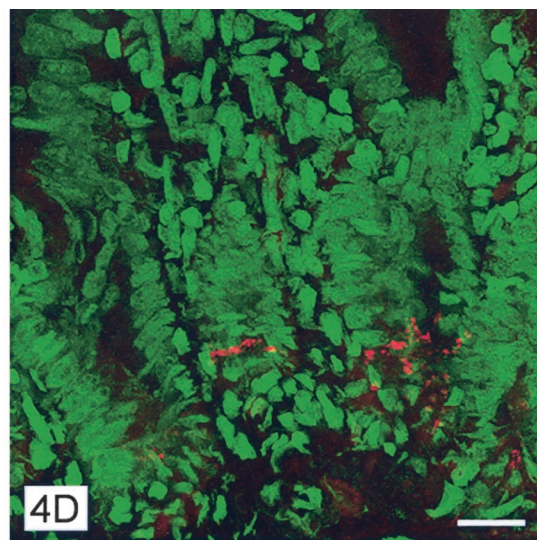
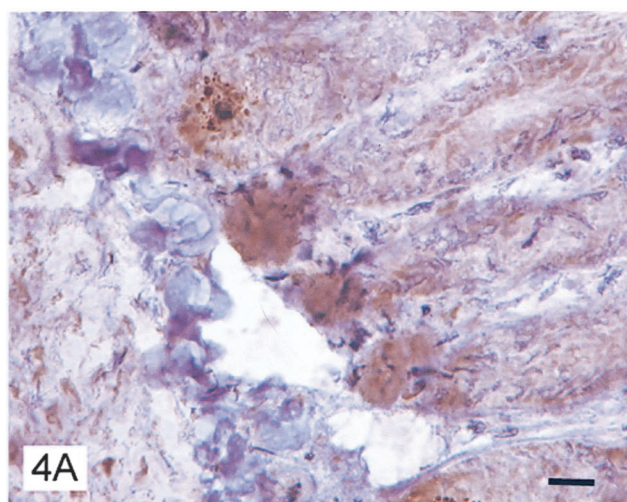


Figure 4. Immunohistochemical reactivity with TLR9 mAb of jejunum epithelial cells from mice 24 hours previously injected intraperitoneally with 1668 CpG-ODN (A) or control AP1-ODN (B) or left untreated (C). **D–F:** Confocal images of Paneth cells of jejunum from mice 24 hours previously treated with CpG-ODN or AP1-ODN or left untreated, respectively. Scale bars: 10 μ m (A–C); 17 μ m (D–F).

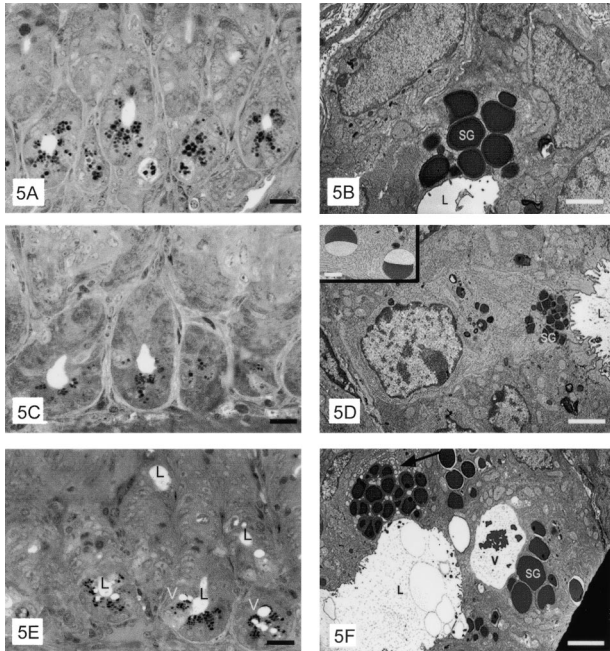


Figure 5. Electron photomicrographs of the bottom of crypts and electron micrographs of Paneth cells from mice untreated (**A, B**) or injected intraperitoneally 3 hours (**B, C**) or 12 hours (**E, F**) previously with 1668 CpG-ODN. Secretory granules (SG), smooth vesicles (arrows), vacuoles (V), and crypt lumen (L) are indicated. Scale bars: 10 μm (**A, C, E**); 1.7 μm (**B**); 2.1 μm (**D**); 3.4 μm (**F**); 1 μm (inset).

ecules. Recently, it has been described the expression in Paneth cells of NOD2³³ which is implicated in lipopolysaccharide recognition. Interestingly, like TLR9, NOD2 appears located in the close proximity of Paneth cell granules.³⁴ Unlike other TLRs, TLR9 expression has been described essentially as intracellular.³⁵ Moreover circumstantial evidence indicated that TLR9 in phagocytic cells, the only cells until recently thought to express TLR9, was present at the endosomal level.³⁶ Because bacterial DNA resides inside the pathogen, destruction of the pathogen's cell wall and release of its DNA is a prerequisite for

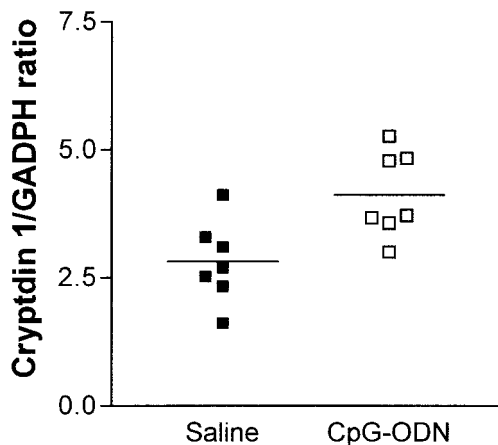


Figure 6. mRNA expression of Paneth cell cryptdin 1 in response to CpG-ODN as quantified by Northern blot analysis. Mice were injected intraperitoneally 3 hours previously with saline or CpG-ODN and then sacrificed. Intestinal crypts were isolated by dissociation of small intestine segments. Quantification was obtained by normalization with GADPH expression. Each point represents one mouse.

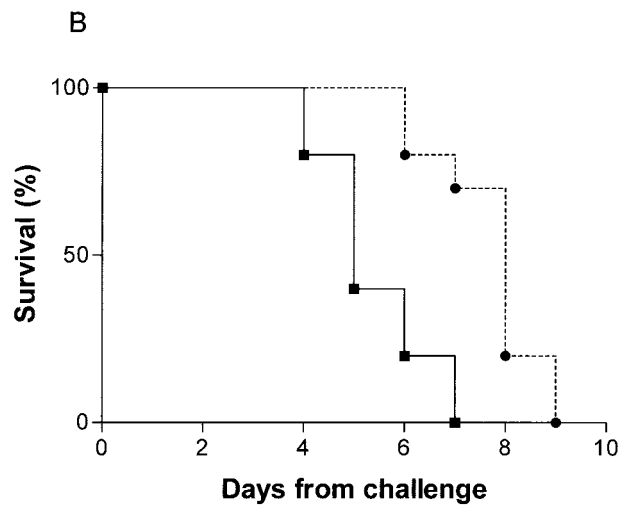
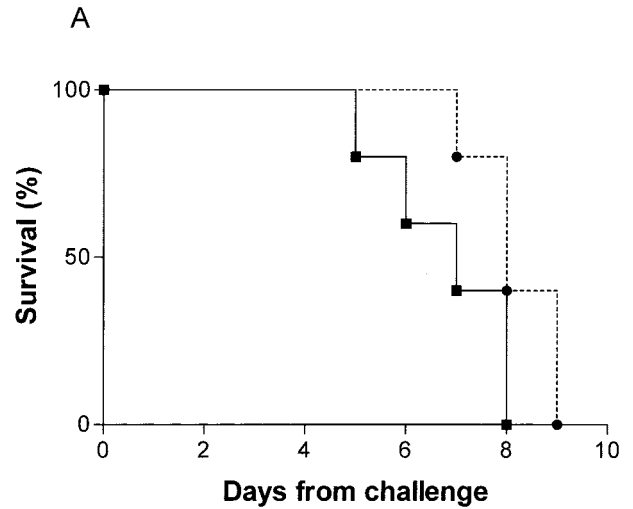


Figure 7. Survival curve after oral challenge with a virulent strain of *S. typhimurium* (ATCC 14028). Mice were inoculated with saline (■) or 1668 CpG-ODN (●) and 3 days later, with 1.6×10^7 (**A**) or 1.6×10^7 (**B**) CFU of bacteria.

TLR9 activation. These processes take place in lysosomes after phagocytosis and endosomal maturation. In phagocytic cells, TLR9 is specifically localized to the cellular sites of ligand liberation. In cells without phagocytic capability, as appears to be the case for Paneth cells, TLR9 is localized on the granules. In these cells, bacterial DNA fragments liberated, for example, by macrophages might be internalized by diffusion and interact with TLR9 on the granule to induce degranulation. Indeed, electron microscopy clearly showed that CpG-ODN treatment induces changes in secretory granules similar to those observed in germ-free mice inoculated with bacteria.¹⁰ The degranulation process was pronounced at 3 hours and 12 hours after CpG treatment, while at 24 hours, granule dimension and morphology were similar to that in untreated and AP1-treated mice, suggesting granule reaccumulation. The decrease in TLR9-positive granules at 24 hours after CpG treatment suggests that the newly formed granules are delayed in re-expressing TLR9, which may require more time for

synthesis. TLR9 expression was decreased even in enterocytes, raising the possibility of degranulation in these cells as well. In fact, it has been reported that certain epithelial cells active genes encoding defensins in response to bacteria,^{37,38} therefore a self-protection mechanism through a direct effect of CpG-ODN on these cells cannot be ruled out.

Intestinal crypts isolated from mice before injection with CpG-ODN revealed an increase in cryptdin 1 mRNA expression, thus supporting the hypothesis that binding of TLR9 by its cognate ligand induces the production of defensins and other molecules from Paneth cells. Moreover, in mice pretreated with CpG-ODN and orally challenged with *S. typhimurium* a significant delay in mortality was observed. To our knowledge this is the first report of CpG-ODN administration by itself increasing survival of mice challenged with an enteric pathogen. The role of defensins in controlling *S. typhimurium* infections had been reported only in mice rendered deficient in enzyme implicated in the processing of intestinal defensins³⁰ or in mice transgenic for expression of a human intestinal defensin.¹⁸ As regards CpG-ODN, it has been reported that CpG-ODN pretreatment reduces the number of *Listeria monocytogenes*, when administered 48 to 96 hours before the challenge with this enteric pathogen, even in mice lacking Peyer's patches.^{39,40} On the basis of these data and considering that defensins are reported to act also indirectly by inducing cytokine and chemokine release,⁴¹ mice were orally challenged with *S. typhimurium* 72 hours after CpG-ODN treatment, but it is plausible that CpG-ODN treatment should reduce susceptibility to infection even in a shorter time. Accordingly for a role of TLR9 signaling on gut protection, recently it has been described the anti-inflammatory effect exerted by probiotic DNA treatment on dextran sodium sulfate-induced murine colitis.⁴²

In our study, CpG-ODNs were delivered intraperitoneally to the gut, and it is unknown whether CpG-containing DNA fragments from luminal bacteria reach Paneth cells under physiological conditions, or, in light of the location of these cells in the deepest layers of the intestinal mucosa, whether this event occurs only on alteration of the mucosa. The presence of TLR9 in Paneth cells might explain the data of Ayabe and colleagues,²⁰ who reported a secretory response by Paneth cells from isolated crypts exposed to gram-positive and gram-negative bacteria, but no secretion of defensins by these cells after exposure to eukaryotic microbial pathogens, such as *Candida albicans*, *Cryptococcus neoformans*, or *Giardia lamblia*. This innate mechanism of protection after exposure to bacteria might be physiologically relevant in protecting crypts. Further studies are needed to assess whether Paneth cell activation through CpG-TLR9 interaction induces secretion of cytokines to coordinate host defenses with other cell types.

Acknowledgments

We thank Mrs. L. Mameli for preparing the manuscript, Mr. L. Losi for preparing electron microscopy samples, and M.M. Scaltrito for microbiological support.

References

1. Porter EM, Bevins CL, Ghosh D, Ganz T: The multifaceted Paneth cell. *Cell Mol Life Sci* 2002, 59:156–170
2. Mathan M, Hughes J, Whitehead R: The morphogenesis of the human Paneth cell. An immunocytochemical ultrastructural study. *Histochemistry* 1987, 87:91–96
3. Bach SP, Renehan AG, Potten CS: Stem cells: the intestinal stem cell as a paradigm. *Carcinogenesis* 2000, 21:469–476
4. Booth C, Potten CS: Gut instincts: thoughts on intestinal epithelial stem cells. *J Clin Invest* 2000, 105:1493–1499
5. Jones DE, Bevins CL: Defensin-6 mRNA in human Paneth cells: implications for antimicrobial peptides in host defense of the human bowel. *FEBS Lett* 1993, 315:187–192
6. Ouellette AJ, Hsieh MM, Nosek MT, Cano-Gauci DF, Huttner KM, Buick RN, Selsted ME: Mouse Paneth cell defensins: primary structures and antibacterial activities of numerous cryptdin isoforms. *Infect Immun* 1994, 62:5040–5047
7. Deckx RJ, Vantrappen GR, Parein MM: Localization of lysozyme activity in a Paneth cell granule fraction. *Biochim Biophys Acta* 1967, 139:204–207
8. Peeters T, Vantrappen G: The Paneth cell: a source of intestinal lysozyme. *Gut* 1975, 16:553–558
9. Senegas-Balas F, Balas D, Verger R, de Caro A, Figarella C, Ferrato F, Lechene P, Bertrand C, Ribet A: Immunohistochemical localization of intestinal phospholipase A2 in rat Paneth cells. *Histochemistry* 1984, 81:581–584
10. Satoh Y, Ishikawa K, Tanaka H, Ono K: Immunohistochemical observations of immunoglobulin A in the Paneth cells of germ-free and formerly-germ-free rats. *Histochemistry* 1986, 85:197–201
11. Taupin D, Ooi K, Yeomans N, Giraud A: Conserved expression of intestinal trefoil factor in the human colonic adenoma-carcinoma sequence. *Lab Invest* 1996, 75:25–32
12. Poulsen SS, Nexø E, Olsen PS, Hess J, Kirkegaard P: Immunohistochemical localization of epidermal growth factor in rat and man. *Histochemistry* 1986, 85:389–394
13. Denhardt DT, Guo X: Osteopontin: a protein with diverse functions. *FASEB J* 1993, 7:1475–1482
14. Qu XD, Lloyd KC, Walsh JH, Lehrer RI: Secretion of type II phospholipase A2 and cryptdin by rat small intestinal Paneth cells. *Infect Immun* 1996, 64:5161–5165
15. Mastly J, Stradley RP: Paneth cell degranulation and lysozyme secretion during acute equine alimentary laminitis. *Histochemistry* 1991, 95:529–533
16. Ganz T: Microbiology: gut defence. *Nature* 2003, 422:478–479
17. Hooper LV, Stappenbeck TS, Hong CV, Gordon JI: Angiogenins: a new class of microbicidal proteins involved in innate immunity. *Nat Immunol* 2003, 4:269–273
18. Salzman NH, Ghosh D, Huttner KM, Paterson Y, Bevins CL: Protection against enteric salmonellosis in transgenic mice expressing a human intestinal defensin. *Nature* 2003, 422:522–526
19. Ghosh D, Porter E, Shen B, Lee SK, Wilk D, Drazba J, Yadav SP, Crabb JW, Ganz T, Bevins CL: Paneth cell trypsin is the processing enzyme for human defensin-5. *Nat Immunol* 2002, 3:583–590
20. Ayabe T, Satchell DP, Wilson CL, Parks WC, Selsted ME, Ouellette AJ: Secretion of microbicidal alpha-defensins by intestinal Paneth cells in response to bacteria. *Nat Immunol* 2000, 1:113–118
21. Belvin MP, Anderson KV: A conserved signaling pathway: the *Drosophila* toll-dorsal pathway. *Annu Rev Cell Dev Biol* 1996, 12:393–416
22. Lemaitre B, Nicolas E, Michaut L, Reichhart JM, Hoffmann JA: The dorsoventral regulatory gene cassette spätzle/Toll/cactus controls the potent antifungal response in *Drosophila* adults. *Cell* 1996, 20:86:973–983
23. Rock FL, Hardiman G, Timans JC, Kastelein RA, Bazan JF: A family of human receptors structurally related to *Drosophila* Toll. *Proc Natl Acad Sci USA* 1998, 95:588–593
24. Ballas ZK, Rasmussen WL, Krieg AM: Induction of NK activity in murine and human cells by CpG motifs in oligodeoxynucleotides and bacterial DNA. *J Immunol* 1996, 157:1840–1845
25. Pisetsky DS: Immune activation by bacterial DNA: a new genetic code. *Immunity* 1996, 5:303–310
26. Akhtar M, Watson JL, Nazli A, McKay DM: Bacterial DNA evokes

- epithelial IL-8 production by a MAPK-dependent, NF-kappaB-independent pathway. *FASEB J* 2003, 17:1319–1321
27. United Kingdom Co-ordinating Committee on Cancer Research (UKCCCR) guidelines for the welfare of animals in experimental neoplasia, ed. 2. *Br J Cancer* 1998, 77:1–10
 28. Dalpke AH, Schafer MKH, Frey M, Zimmermann S, Tebbe J, Weihe E, Heeg K: Immunostimulatory CpG-DNA activates murine microglia. *J Immunol* 2002, 168:4854–4863
 29. Bauer S, Kirschning CJ, Hacker H, Redecke V, Hausmann S, Akira S, Wagner H, Lipford GB: Human TLR9 confers responsiveness to bacterial DNA via species-specific CpG motif recognition. *Proc Natl Acad Sci USA* 2001, 98:9237–9242
 30. Wilson CL, Ouellette AJ, Satchell DP, Ayabe T, Lopez-Boado YS, Stratman JL, Hultgren SJ, Matrisian LM, Parks WC: Regulation of intestinal alpha-defensin activation by the metalloproteinase matrilysin in innate host defense. *Science* 1999, 286:113–117
 31. Cario E, Rosenberg IM, Brandwein SL, Beck PL, Reinecker HC, Podolsky DK: Lipopolysaccharide activates distinct signaling pathways in intestinal epithelial cell lines expressing Toll-like receptors. *J Immunol* 2000, 164:966–972
 32. Cario E, Podolsky DK: Differential alteration in intestinal epithelial cell expression of toll-like receptor 3 (TLR3) and TLR4 in inflammatory bowel disease. *Infect Immun* 2000, 68:7010–7017
 33. Lala S, Ogura Y, Osborne C, Hor SY, Bromfield A, Davies S, Ogunbiyi O, Nunez G, Keshav S: Crohn's disease and the NOD2 gene: a role for Paneth cells. *Gastroenterology* 2003, 125:47–57
 34. Ogura Y, Lala S, Xin W, Smith E, Dowds TA, Chen FF, Zimmermann E, Tretiakova M, Cho JH, Hart J, Greenson JK, Keshav S, Nunez G: Expression of NOD2 in Paneth cells: a possible link to Crohn's ileitis. *Gut* 2003, 52:1591–1597
 35. Ahmad-Nejad P, Hacker H, Rutz M, Bauer S, Vabulas RM, Wagner H: Bacterial CpG-DNA and lipopolysaccharides activate Toll-like receptors at distinct cellular compartments. *Eur J Immunol* 2002, 32:1958–1968
 36. Hemmi H, Takeuchi O, Kawai T, Kaisho T, Sato S, Sanjo H, Matsumoto M, Hoshino K, Wagner H, Takeda K, Akira S: A Toll-like receptor recognizes bacterial DNA. *Nature* 2000, 408:740–745
 37. Diamond G, Bevins CL: Beta-defensins: endogenous antibiotics of the innate host defense response. *Clin Immunol Immunopathol* 1998, 88:221–225
 38. Bals R, Wang X, Meegalla RL, Wattler S, Weiner DJ, Nehls MC, Wilson JM: Mouse beta-defensin 3 is an inducible antimicrobial peptide expressed in the epithelia of multiple organs. *Infect Immun* 1999, 67:3542–3547
 39. Krieg AM, Love-Homan L, Yi AK, Harty JT: CpG DNA induces sustained IL-12 expression in vivo and resistance to *Listeria monocytogenes* challenge. *J Immunol* 1998, 161:2428–2434
 40. Ray NB, Krieg AM: Oral pretreatment of mice with CpG DNA reduces susceptibility to oral or intraperitoneal challenge with virulent *Listeria monocytogenes*. *Infect Immun* 2003, 71:4398–4404
 41. Lin PW, Simon PO, Gewirtz AT, Neish AS, Ouellette AJ, Madara JL, Lencer WI: Paneth cell cryptidins act in vitro as apical paracrine regulators of the innate inflammatory response. *J Biol Chem* 2004, 279:1182–1200
 42. Rachmilewitz D, Katakura K, Karmeli F, Hayashi T, Reinus C, Rudensky B, Akira S, Takeda K, Lee J, Takabayashi K, Raz E: Toll-like receptor 9 signaling mediates the anti-inflammatory effects of probiotics in murine experimental colitis. *Gastroenterology* 2004, 126:520–528